

DAHLGREN DIVISION
NAVAL SURFACE WARFARE CENTER

Dahlgren, Virginia 22448-5100



NSWCDD/TR-97/75

**POTENTIAL MEASUREMENT ERRORS INDUCED BY
ATMOSPHERIC REFRACTION**

BY JAMES KEENER

THEATER WARFARE SYSTEMS DEPARTMENT

MARCH 1997

Approved for public release; distribution is unlimited.

19980423 015

DTIC QUALITY INSPECTED 3

REPORT DOCUMENTATION PAGEForm Approved
OMB No. 0704-0188

Public reporting burden for this collection of information is estimated to average 1 hour per response, including the time for reviewing instructions, search existing data sources, gathering and maintaining the data needed, and completing and reviewing the collection of information. Send comments regarding this burden or any other aspect of this collection of information, including suggestions for reducing this burden, to Washington Headquarters Services, Directorate for Information Operations and Reports, 1215 Jefferson Davis Highway, Suite 1204, Arlington, VA 22202-4302, and to the Office of Management and Budget, Paperwork Reduction Project (0704-0188), Washington, DC 20503.

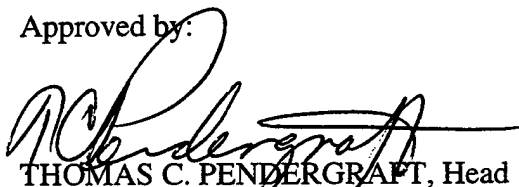
1. AGENCY USE ONLY (Leave blank)		2. REPORT DATE March 1997	3. REPORT TYPE AND DATES COVERED Final	
4. TITLE AND SUBTITLE Potential Measurement Errors Induced by Atmospheric Refraction			5. FUNDING NUMBERS	
6. AUTHOR(s) James Keener				
7. PERFORMING ORGANIZATION NAME(S) AND ADDRESS(ES) Commander Naval Surface Warfare Center Dahlgren Division (Code T41) 17320 Dahlgren Road Dahlgren, VA 22448-5100			8. PERFORMING ORGANIZATION REPORT NUMBER NSWCDD/TR-97/75	
9. SPONSORING/MONITORING AGENCY NAME(S) AND ADDRESS(ES) Office of Naval Research Crystal Square 2 Arlington, VA 22217			10. SPONSORING/MONITORING AGENCY REPORT NUMBER	
11. SUPPLEMENTARY NOTES				
12a. DISTRIBUTION/AVAILABILITY STATEMENT Approved for public release; distribution is unlimited.			12b. DISTRIBUTION CODE	
13. ABSTRACT (Maximum 200 words) This report outlines the potential significance of atmospheric refraction and trapping in the measurement of low-altitude targets by airborne sensors. The report addresses two problems: first, the magnitude of potential position errors attributed to atmospheric refraction and trapping; and second, the determination of a seeker's field of view and the necessary measurement accuracy of an airborne radar to hand over a target to an intercept missile. In the discussion of the second problem, a criterion is established for comparison of the magnitude of measurement errors associated with atmospheric refraction.				
14. SUBJECT TERMS index of refraction, surface-based duct, elevated duct, atmospheric refraction, trapping, interceptor field-of-view, Snell's law, Precision Track and Illuminate Radar, PTIR			15. NUMBER OF PAGES 36	
			16. PRICE CODE	
17. SECURITY CLASSIFICATION OF REPORTS UNCLASSIFIED	18. SECURITY CLASSIFICATION OF THIS PAGE UNCLASSIFIED	19. SECURITY CLASSIFICATION OF ABSTRACT UNCLASSIFIED	20. LIMITATION OF ABSTRACT UL	

FOREWORD

A concept using an air-directed, surface-to-air missile is being considered by the Navy to extend the engagement range of surface ships. The airborne unit performs search, track, and illumination functions. Tracking is considered successful if the system is able to properly hand over a target to terminal missile guidance. However, the success of this handover relies on the angular accuracy of the airborne radar. This report examines the potential significance of abnormally large gradients in the vertical profile of atmospheric refraction. The report is specifically concerned with how these abnormally large gradients affect the measurement accuracy of the airborne sensors attempting to track low-altitude targets, e.g., low-flying cruise missiles.

This report has been reviewed by B. J. Barnes, T41, Self Defense Sensors Branch, and S. Koch, T40, Theater Warfare Sensors Division.

Approved by:



THOMAS C. PENDERGRAFT, Head
Theater Warfare Systems Department

CONTENTS

<u>Chapter</u>	<u>Page</u>
INTRODUCTION	1
DUCTING CLIMATOLOGY	1
THEORETICAL REFRACTION	2
POTENTIAL POSITION ERRORS	3
SIGNIFICANCE OF REFRACTION	4
MISSILE SEEKER FIELD OF VIEW	4
ESTIMATE OF REQUIRED MEASUREMENT ACCURACY	5
CONCLUSIONS	7
DISTRIBUTION	(1)

ILLUSTRATIONS

<u>Figure</u>		<u>Page</u>
1	SCHEMATIC REPRESENTATION OF ATMOSPHERICALLY INDUCED BENDING OF EM WAVES.....	9
2	ILLUSTRATION OF GEOMETRY USED TO OBTAIN RESULTS	10
3	APPROACH ANGLES OF EM WAVES RELATIVE TO DUCT CEILING FOR SURFACE TARGETS: 50 m DUCT CEILING	11
4	APPROACH ANGLES OF EM WAVES RELATIVE TO DUCT CEILING FOR SURFACE TARGETS: 1000 M DUCT CEILING.....	12
5	APPROACH ANGLES OF EM WAVES RELATIVE TO DUCT CEILING FOR SURFACE TARGETS: 2000 m DUCT CEILING	13
6	APPROACH ANGLES OF EM WAVES RELATIVE TO DUCT CEILING FOR SURFACE TARGETS: 3000 m DUCT CEILING	14
7	APPROACH ANGLES AND PATH LENGTHS: DUCT CEILING OF 50 m AND SENSOR ALTITUDE OF 5000 m.....	15
8	APPROACH ANGLES AND PATH LENGTHS: DUCT CEILING OF 2000 m AND SENSOR ALTITUDE OF 5000 m.....	16
9	APPROACH ANGLES AND PATH LENGTHS: DUCT CEILING OF 50 m AND SENSOR ALTITUDE OF 3000 m.....	17
10	APPROACH ANGLES AND PATH LENGTHS: DUCT CEILING OF 2000 m AND SENSOR ALTITUDE OF 3000 m.....	18
11	MODIFIED REFRACTION PROFILES: "A" IS A REALISTIC PROFILE AND "B" IS AN ALTERED PROFILE USED IN THIS REPORT	19
12	VERTICAL POSITION ERRORS INDUCED BY REFRACTION: N "OFFSET" OF 60 N UNITS	20

ILLUSTRATIONS (Continued)

<u>Figure</u>		<u>Page</u>
13	VERTICAL POSITION ERRORS INDUCED BY REFRACTION: N "OFFSET" OF 40 N UNITS	21
14	VERTICAL POSITION ERRORS INDUCED BY REFRACTION: N "OFFSET" OF 20 N UNITS	22
15	INTERCEPTOR SEEKER FIELD OF VIEW	23
16	RATIO OF ALTITUDE ERRORS TO SEEKER FIELD OF VIEW (SEEKER BEAMWIDTH = 8°: ACQUISITION RANGE = 9 km	24
17	RATIO OF ALTITUDE ERRORS TO SEEKER FIELD OF VIEW (SEEKER BEAMWIDTH = 4°: ACQUISITION RANGE = 5 km	25
18	SENSOR ANGULAR ACCURACY	26
19	ANGULAR ERROR INDUCED BY ATMOSPHERIC REFRACTION.....	27

TABLES

<u>Table</u>		<u>Page</u>
1	CLIMATOLOGICAL DATA USING RADIOSONDE INFORMATION	2

INTRODUCTION

This technical report outlines the potential significance of atmospheric refraction and trapping on measurement accuracy of low altitude targets by airborne sensors. Addressed is the magnitude of potential position errors attributed to atmospheric refraction and trapping. Also presented is a short determination of a seeker's field of view and the necessary measurement accuracy of an airborne radar to handover a target to an intercept missile. This section establishes a criterion for which to compare the magnitude of measurement errors associated with atmospheric refraction.

DUCTING CLIMATOLOGY

The index of refraction of a standard atmosphere decreases exponentially with height, hence bending of electromagnetic (EM) waves is present but typically corrected in existing equations by modifying the earth's radius with a factor of 4/3. However, layers of abnormally large vertical gradients in the index of refraction relative to the ambient atmosphere form ducts.

Two categories of ducts will be addressed in this report: surface based and elevated. Surface based ducts are most often less than 40 m deep and found at altitudes below 100 m. Elevated ducts are most often 200 - 300 m deep and can be present at virtually any altitude, but climatology suggests typical altitudes are between 1000 and 2000 m Above Ground Level (AGL). Table 1 list the annual averages of ceiling heights, thickness, and duct strength measured at five locations worldwide. Climate data was obtained from the Naval Command and Control Ocean Surveillance Center, Research, Development, Test and Evaluation (NRaD). The total decrease of the modified index of refraction, M , and the total decrease of the refractivity within the layer are also listed; the numbers shown include the gradients found within the standard atmosphere. The total N units were obtained from the total M units using the relationship¹

$$\frac{dN}{dh} = \frac{dM}{dh} - 0.157,$$

where dh is the duct thickness.

¹ *Engineer's Refractive Effects Prediction System*, Naval Command, Control, and Ocean Surveillance Center RDT&E Division, Technical Document 2648, May 1994.

TABLE 1. CLIMATOLOGICAL DATA USING RADIOSONDE INFORMATION

Radiosonde Location	Duct Top (m)	Duct Thickness (m)	Total M units	Total N units
Pyongyang	2007	126	-36.9	-56.7
Osan Air Base	1394	89	-10.6	-24.5
Belgrade	1611	99	-11.8	-27.4
Wallops Island	1472	118	-13.9	-32.4
Hilo, Hawaii	2270	170	-19.2	-45.9
Kuwait	1540	144	-25.0	-47.6

THEORETICAL REFRACTION

Skolnik (1990)² suggests that the angle of approach to the duct ceiling of EM waves determines the significance of refraction and trapping. Following Figure 1, if the angle of the EM wave relative to the duct ceiling (i.e., the approach angle) is approximately 1.5° or less, refraction is a problem and trapping of EM waves within the duct possible. If the approach angle ranges between 1.5° and 5°, trapping is not likely but bending of EM waves may lead to unacceptable measurement errors. When the approach angle is greater than 5°, the bending angle becomes insignificant and ignored in most cases with bending approaching values less than 0.1 mr. It should be noted that erroneous measurements caused by refraction is not unique to airborne radars. The refraction examined for an elevated sensor can also be applied to surface based radars.

Figure 2 shows the geometry involved with computing the angle of elevation relative to the duct ceiling (i.e., the approach angle) when considering a surface target, e.g., a low flying cruise missile. Figures 3, 4, 5, and 6 show approach angles relative to the duct ceilings as a function of sensor-to-target range and sensor altitude for a surface target with ceilings at 50, 1000, 2000, and 3000 m AGL. The horizontal lines represent approach angles that are less than 1.5°, at which angle both trapping and refraction can be potential problems. The slanted lines represent the zone in which refraction is the only potential problem, and the vertical lines represent the zone in which refraction is not significant. The target ranges for which refraction and trapping is not an issue is essentially the same for each of the four duct ceilings with the 5° angle of approach not fluctuating considerably. The region of potential refraction is much greater for a surface based duct, but, as will be shown later, the magnitude of measurement errors caused by a surface duct are insignificant.

Having obtained the approach angle, Snell's law,

$$n_1 \sin(\theta_1) = n_2 \sin(\theta_2), \quad (1)$$

² Skolnik, Merrill, *Radar Handbook*, McGraw-Hill, 1990, pp. 25-35.

where the incident angle $\theta_1 = \pi - \alpha$,

can be used to obtain the refraction angle, θ_2 , and with n_1 and n_2 , the index of refraction above and below the duct altitude. It has been assumed that the ducting layer can be considered as a discontinuity in the atmospheric index of refraction $n_2 - n_1$ or an "offset." Therefore the angle of refraction is,

$$\theta_2 = \sin^{-1}\left(\frac{n_1}{n_2}\sin(\pi - \alpha)\right). \quad (2)$$

The magnitude of the position error, shown in Figure 1, is then

$$\Delta P = (\theta_2 - (\pi - \alpha))(r), \quad (3)$$

with r , the duct-to-target path length, which is also shown in Figure 1. The position errors will be referred to as altitude errors since the errors are primarily in the vertical plane at the ranges considered.

POTENTIAL POSITION ERRORS

In this section, the potential measurement errors associated with refraction will be examined for surface based and elevated ducts. Two sensor altitudes are considered.

Figures 7 through 10 show the approach angles and path lengths, as a function of target altitude and ground range for sensor altitudes of 3000 and 5000 m and duct ceilings of 50 and 2000 m. The equations shown in Figure 2 were modified slightly to include target altitudes above the surface. The solid lines in each figure represent contours of constant approach angles at 0.2° intervals, and the path lengths are represented by the dashed lines at intervals that differ for each figure. When the duct ceilings are higher, the approach angles are slightly greater. For instance, when detecting a surface target at 120 km, the approach angles of a 50 m duct are only approximately 0.9° and 1.3° for sensor altitudes of 3000 and 5000 m, respectively. When the duct ceiling is increased to 2000 m, the approach angles increase to approximately 2.4° and 2.6° for 3000 and 5000 m sensor altitudes, respectively. From this one may falsely conclude that refraction errors are greater in the presence of a surface based duct. However, the path lengths associated with detection in a surface based duct are much smaller than for an elevated duct. Again, looking at a 120 km surface target, the path lengths are only 1.6 km for the surface based duct and 55 km for the 2000 m duct. As a result, the position error of a low altitude target will be greater with the existence of higher altitude ducts.

Figure 11 shows a conceptual model of an M profile used to obtain the results shown in this report. The profile labeled A is an illustration of an actual profile with a relative duct thickness of approximately $h_5 - h_2$ and relative M decrease or "offset" within the layer of $2.5 M_0$.

The profile labeled B is the conceptual M profile used in the present analyses. The M "offset" is the same but is now assumed to have zero thickness, in order to simplify computations. Profiles A and B will produce essentially the same total ray bending. Also, the conceptual profile has no thickness and will, therefore, not be responsible for the trapping of EM waves.

Figures 12, 13, and 14 show contoured altitude errors at 20 m intervals as a function of ground range and target altitude for a sensor altitude of 5000 m and index of refraction "offsets" of 60, 40, and 20 N units; these "offsets" are comparable to those listed in Table 1. The duct ceiling has been chosen to be 2000 m, which is also similar to the climatology shown in Table 1 and is considered a near worst case scenario. Shown in the figures are target ground ranges of 100 to 185 km, and target altitudes from the surface up to the duct ceiling. It is assumed that there are no measurement errors of targets above the duct.

Maximum errors shown in the three figures are expectedly associated with an N "offset" of 60 N units. The maximum error for this refractivity gradient is 210 m at a ground range of 180 km and a target altitude of 1200 m. Reducing the N "offset" to 40 N units reduces the maximum position error from 210 to approximately 150 m. Reducing the N "offset" even further to 20 N units decreased the maximum error to only approximately 60 m. When a target is at a ground range of 100 km or less, the altitude errors are essentially negligible for all ducts considered here.

When a surfaced based duct was considered, the magnitudes of the position errors ranged from a minimum of approximately 0 to a maximum of only about 12 m. Even though, the approach angles are relatively small, hence large bending, at the ranges discussed here, the duct-to-target path lengths were very short, hence the position errors are small relative to those shown in Figures 12, 13, and 14.

SIGNIFICANCE OF REFRACTION

This section roughly estimates a seeker's field of view with the intent of establishing a criterion for which to compare the magnitude of the measurement errors created by atmospheric refraction of the radar waves. Also presented is an estimate of the required angular accuracy of an airborne sensor to perform a satisfactory single beam handover of a target to an intercept missile that is assumed to lack scan capability. The position error, ΔP , can be used to approximate an added angular error term.

MISSILE SEEKER FIELD OF VIEW

The spatial extent of the 3 dB beamwidth of a missile seeker is considered here as the seeker's field of view (FOV). Figure 15 shows the FOV as a function of interceptor acquisition range for beamwidths of 4, 6, 8, and 10°. For example, an 8° beamwidth and an acquisition range

of 9 km leads to a 1250 m seeker FOV. Figure 16 shows the ratio of the position errors in Figure 15 to the 1250 m seeker FOV. The percent of the altitude error at 120 km is only 18.4% of the seeker's FOV. On the other hand, as shown in Figure 17, when we consider an acquisition range of only 5 km and a seeker beamwidth of 4° , the FOV is approximately 300 m making the maximum percent of the altitude error nearly 77% of the seeker's FOV. In either case, handover ranges of less than 150 km, provide errors due to the extreme ducting at 2000 m of less than half the seeker FOV. For example, at 120 km, the altitude errors are only 7% and 25% of the seeker FOV for the 8° and 4° beamwidths, respectively. The significance of the altitude error is clearly dependent upon the acquisition range and seeker beamwidth of the interceptor, and target range, with little dependence on target altitude.

ESTIMATE OF REQUIRED MEASUREMENT ACCURACY

Satisfactory missile guidance is defined in this report as the radar detection of a threat within the 3 dB beamwidth of a missile seeker (i.e., the missile seeker's FOV) when a handover is attempted. For success at handover the spatial extent of the seeker's FOV must compensate for position errors of a threat as a result of pointing errors of the seeker and radar measurement errors. Seeker scan capabilities are not considered. Further, it is assumed for simplicity that the position of the intercept missile is known perfectly. Using only the three sigma case,

$$R_I \phi_{skr} \geq 3\sigma_{pos} \quad (4)$$

where R_I is the interceptor-to-threat range, ϕ_{skr} the seeker 3 dB beamwidth, and σ_{pos} is the total measured position error of the threat. In this work,

$$\sigma_{pos} = \sigma_{sen} + \sigma_{lat}, \quad (5)$$

where σ_{sen} is the pointing error associated with the pointing accuracy of the system sensors, σ_{lat} is the pointing error associated with temporal latency of the system.

The pointing error attributed to latency is a function of threat acceleration, data link latency, and prediction filter parameters, e.g., update rate, threat maneuver capability, etc. Latency related errors are beyond the scope of this report, and to simplify discussion it will be ignored.

In Equation (2), the sensor pointing error is

$$\sigma_{sen} = \sqrt{\sigma_{rad}^2 + R_I^2 \sigma_{skr}^2} \quad (6)$$

with σ_{rad} the position accuracy of target measurements made by the Precision Track and Illuminate Radar (PTIR), σ_{skr} the angular pointing accuracy of the intercept missile seeker. For the purposes of this report, the missile seeker pointing error can be approximated as 0.012 radians which consists of the following: initial alignment, quantization accuracy, uplink

quantization accuracy, and platform drift rate (error caused by drift assumes a 100 s time of flight). The radar angular measurement errors in azimuth and elevation is

$$\sigma_{rad} = R_R \sigma_{ang} , \quad (7)$$

with σ_{ang} the angular measurement accuracy (i.e., azimuth and elevation and R_R the radar-to-target range). Clutter rejection requirements will likely lead to a range resolution, hence range error, negligibly small relative to the angular accuracy. The angular accuracy of the radar can be divided into two parameters, the system accuracy and atmospheric contribution to the error. Therefore,

$$\sigma_{ang} = \sigma_{sys} + \sigma_{atm}$$

with σ_{sys} including the beamwidths, filtered angular covariances, or beam splitting accuracy.

The errors attributed to atmospheric phenomena can be expressed as

$$\sigma_{atm} = \sqrt{\sigma_{trap}^2 + \sigma_{ref}^2} ,$$

where σ_{trap} is the pointing error due to duct trapping near the surface of the EM waves at relatively long ranges, and σ_{ref} is error caused by refraction of the radar wave. The error produced by trapping at the surface has not been a focus of this report and specific examples were not presented. As mentioned, trapping is considerably more complicated than error due to refraction since it becomes a function of not only approach angles to a duct but also radar frequency. For simplicity we will assume for this work that error due to trapping is negligibly small. Angular error due to refraction is

$$\sigma_{ref} = \frac{\sigma_{\Delta P}}{R_R} \approx \frac{\Delta P}{R_R} ,$$

where $\sigma_{\Delta P}$ is the one sigma of the position error associated with refraction. However, for specific examples, such as those examined in this report, the error is essentially the position error, ΔP , computed earlier and illustrated in Figure 1. Finally, the radar measurement accuracy becomes

$$\sigma_{rad}^2 = (R_R (\sigma_{sys} + \frac{\Delta P}{R_R}))^2 . \quad (9)$$

The total measurement accuracy of the target's position becomes

$$\sigma_{pos} = \sqrt{R_I^2 \sigma_{skr}^2 + (R_R (\sigma_{sys} + \frac{\Delta P}{R_R}))^2} . \quad (10)$$

Substituting σ_{pos} into Equation (1) yields

$$R_I \phi_{skr} \geq 3 \sqrt{R_I^2 \sigma_{skr}^2 + (R_R (\sigma_{sys} + \frac{\Delta P}{R_R}))^2}. \quad (11)$$

Substituting the seeker angular accuracy error of 0.012 rad and solving for the angular accuracy of the radar system,

$$\sigma_{sys} \leq \frac{1}{R_R} \sqrt{\frac{1}{9} (R_I \phi_{skr})^2 - (R_I 0.012)^2} - \frac{\Delta P}{R_R} \quad (12)$$

If measurements are made in a standard atmosphere, the second term in Equation (12) is zero, leaving only the magnitude of the first term determining the necessary angular accuracy of the system to perform a successful handover. Figure 18 shows the angular accuracy as a function of R_R for several seeker beamwidths and missile-to-target ranges, if refraction is not a factor. Note that if the seeker pointing error is greater than one-ninth the seeker beamwidth, a single beam handover is not possible and seeker scanning will be necessary.

The second term or the atmospheric refraction term places a greater restriction on the accuracy of the radar system. Recall, that the position error, ΔP , is a function of target altitude and range. Figure 19 shows the magnitude of the angular error associated with refraction as a function of target altitude and ground range. The errors are computed for the sensor altitude and duct ceiling height of 5000 m and 2000 m, respectively. The magnitude of the errors range from 0° at the duct ceiling to 0.06° at a range of 180 km and target altitude of approximately 1200 m. Again, the relative significance of angular errors is dependent upon the interceptor acquisition range and seeker beamwidth, i.e., seeker field of view.

CONCLUSIONS

Within this report, refraction of radar waves was addressed with the intent of providing an approximate effect elevated and surface ducts will have on measurement accuracy of low altitude targets with an airborne sensor. It was shown that refraction associated with elevated ducts is not to be ignored. However, the magnitude of the refraction associated with elevated ducts is dependent upon a multitude of parameters, such as sensor altitude, target altitude, duct ceiling height, duct strength, and target ground range. In addition, the significance of the measurement errors associated with refraction is dependent upon the interceptor acquisition range and seeker beamwidth. Handover success ultimately depends on the radar angular accuracy necessary to perform a successful handover of a target to the intercept missile.

Of the parameters addressed, only the existence of a duct, its strength and altitude, will be difficult to ascertain in real time. Because of the complexity of the atmosphere, atmospheric

measurements in real time will likely not provide information to determine perfectly the error associated with ducting. However, measurements may provide an operator with some confidence that atmospheric refraction is or is not a potential threat to achieving a successful mission.

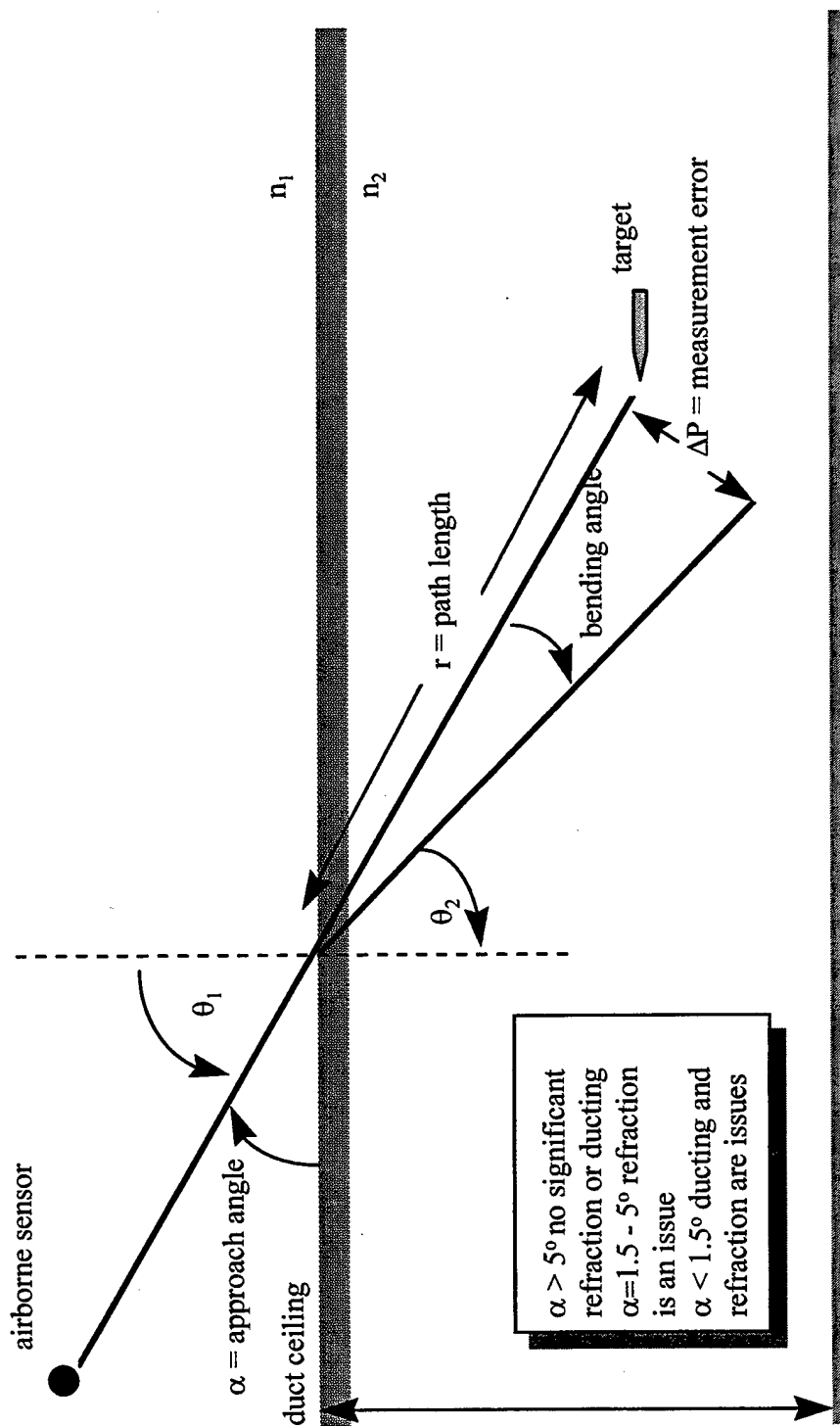


FIGURE 1. SCHEMATIC REPRESENTATION OF ATMOSPHERICALLY INDUCED BENDING OF EM WAVES

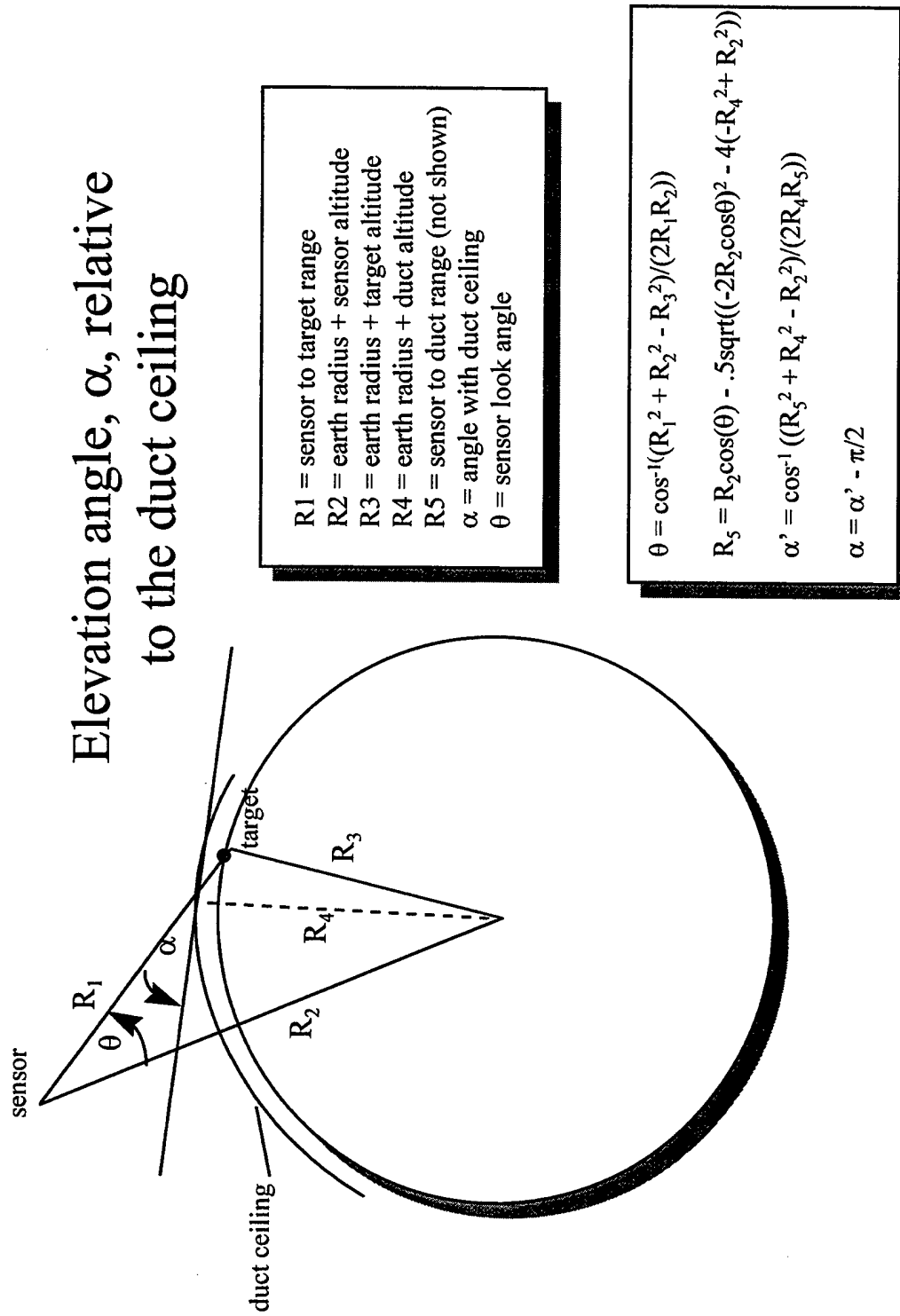


FIGURE 2. ILLUSTRATION OF GEOMETRY USED TO OBTAIN RESULTS

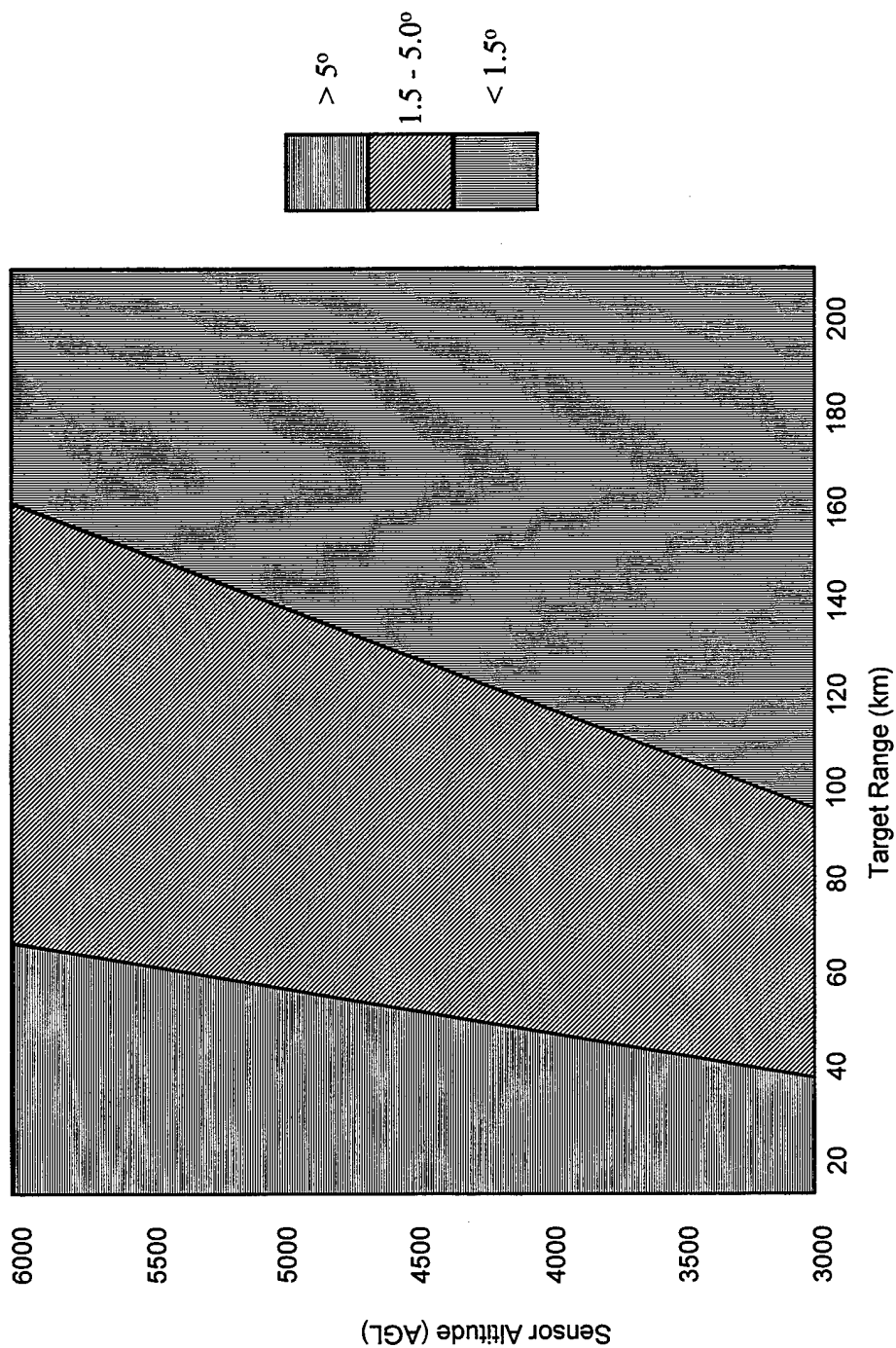


FIGURE 3. APPROACH ANGLES OF EM WAVES RELATIVE TO DUCT
CEILING FOR SURFACE TARGETS: 50 m DUCT CEILING

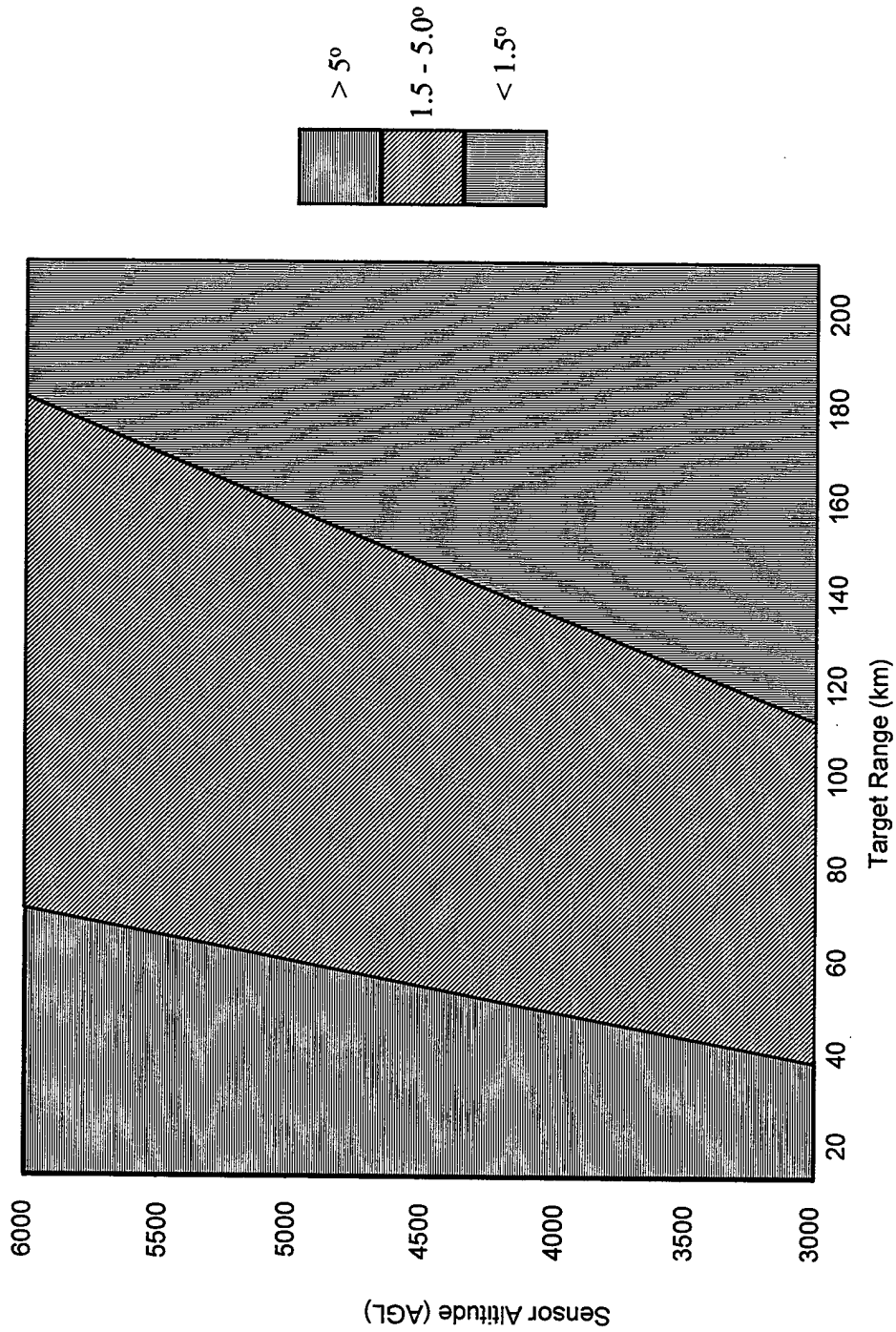


FIGURE 4. APPROACH ANGLES OF EM WAVES RELATIVE TO DUCT CEILING FOR SURFACE TARGETS: 1000 m DUCT CEILING

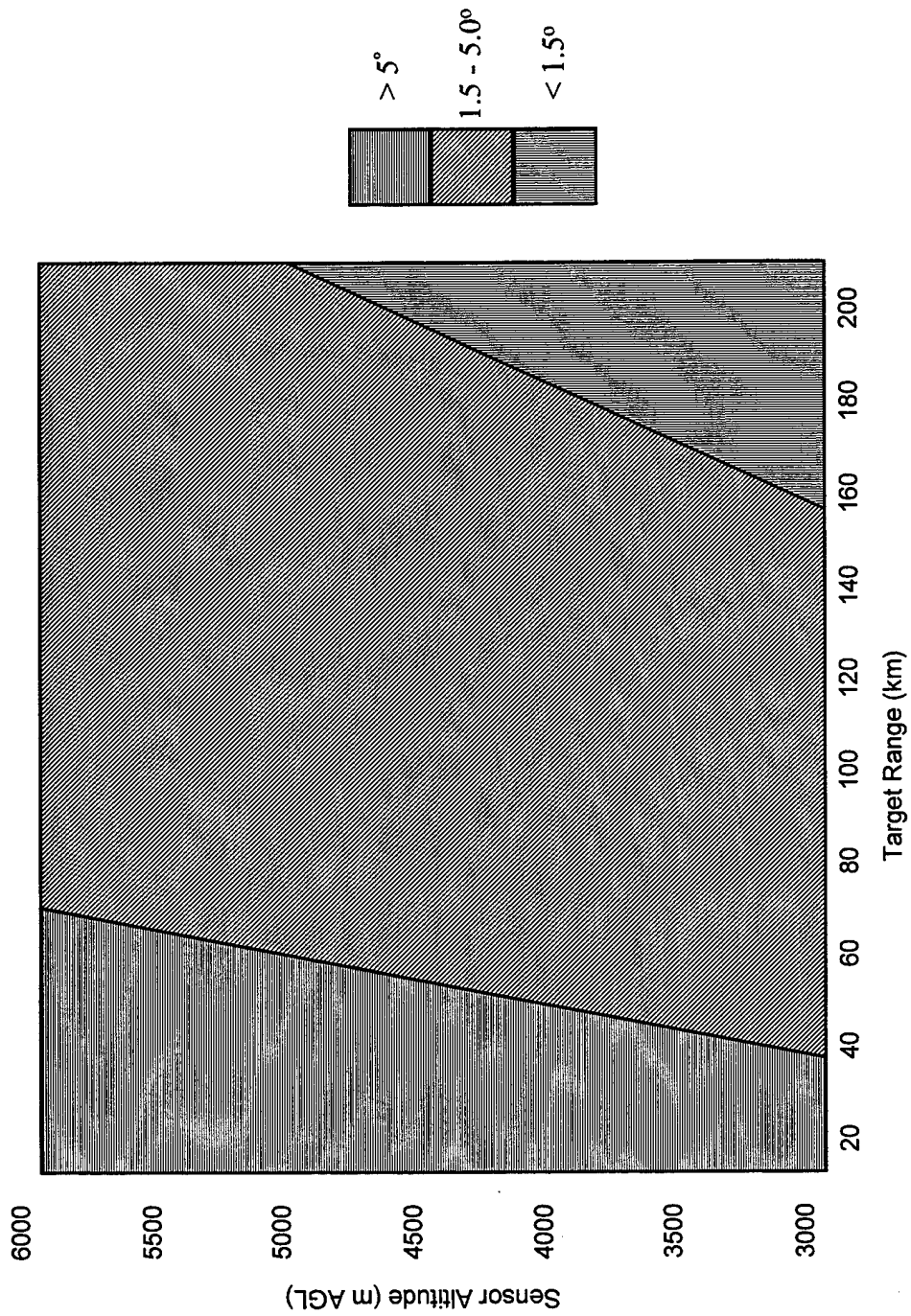


FIGURE 5. APPROACH ANGLES OF EM WAVES RELATIVE TO DUCT CEILING
FOR SURFACE TARGETS: 2000 m DUCT CEILING

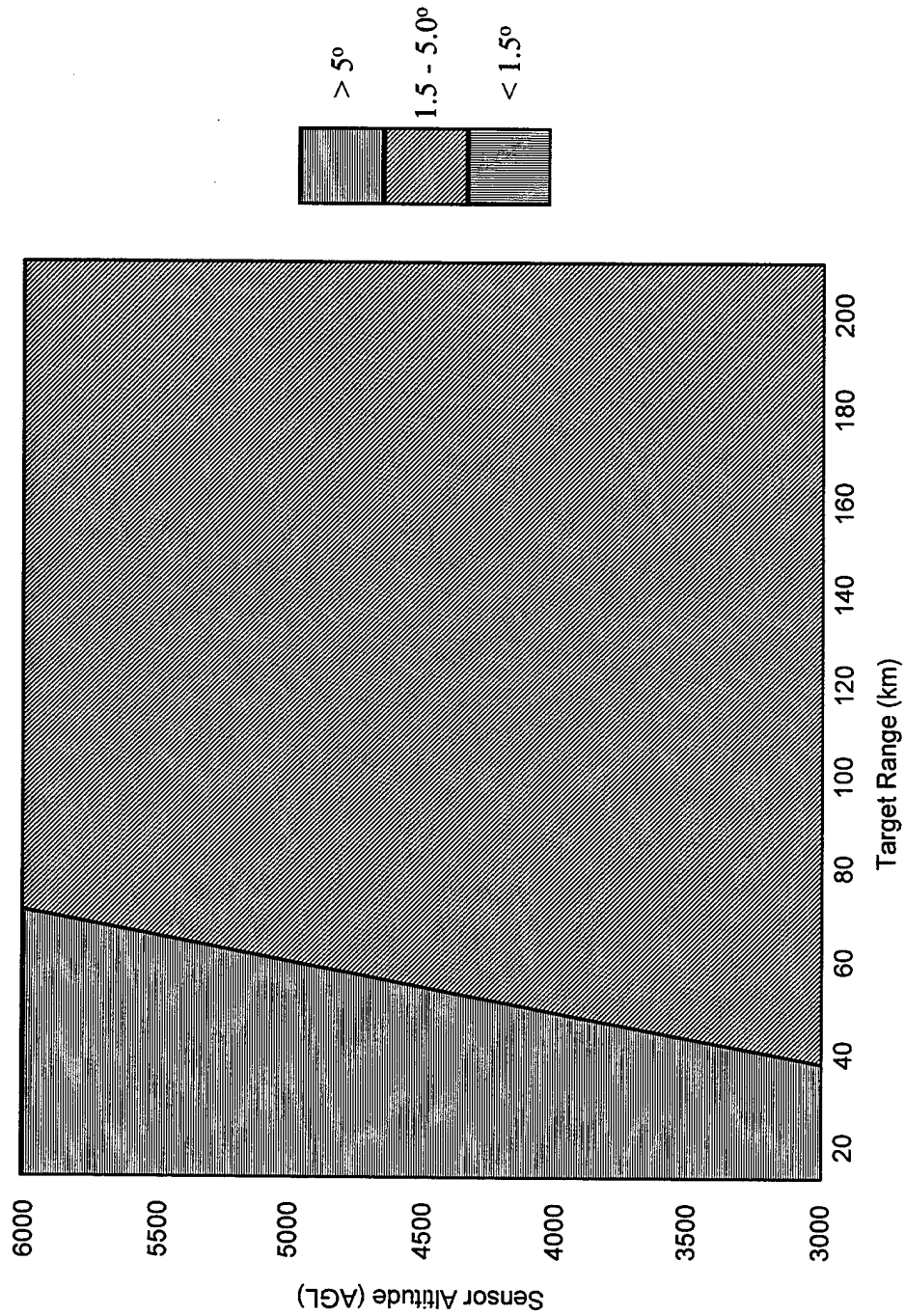


FIGURE 6. APPROACH ANGLES OF EM WAVES RELATIVE TO DUCT CEILING
FOR SURFACE TARGETS: 3000 m DUCT CEILING

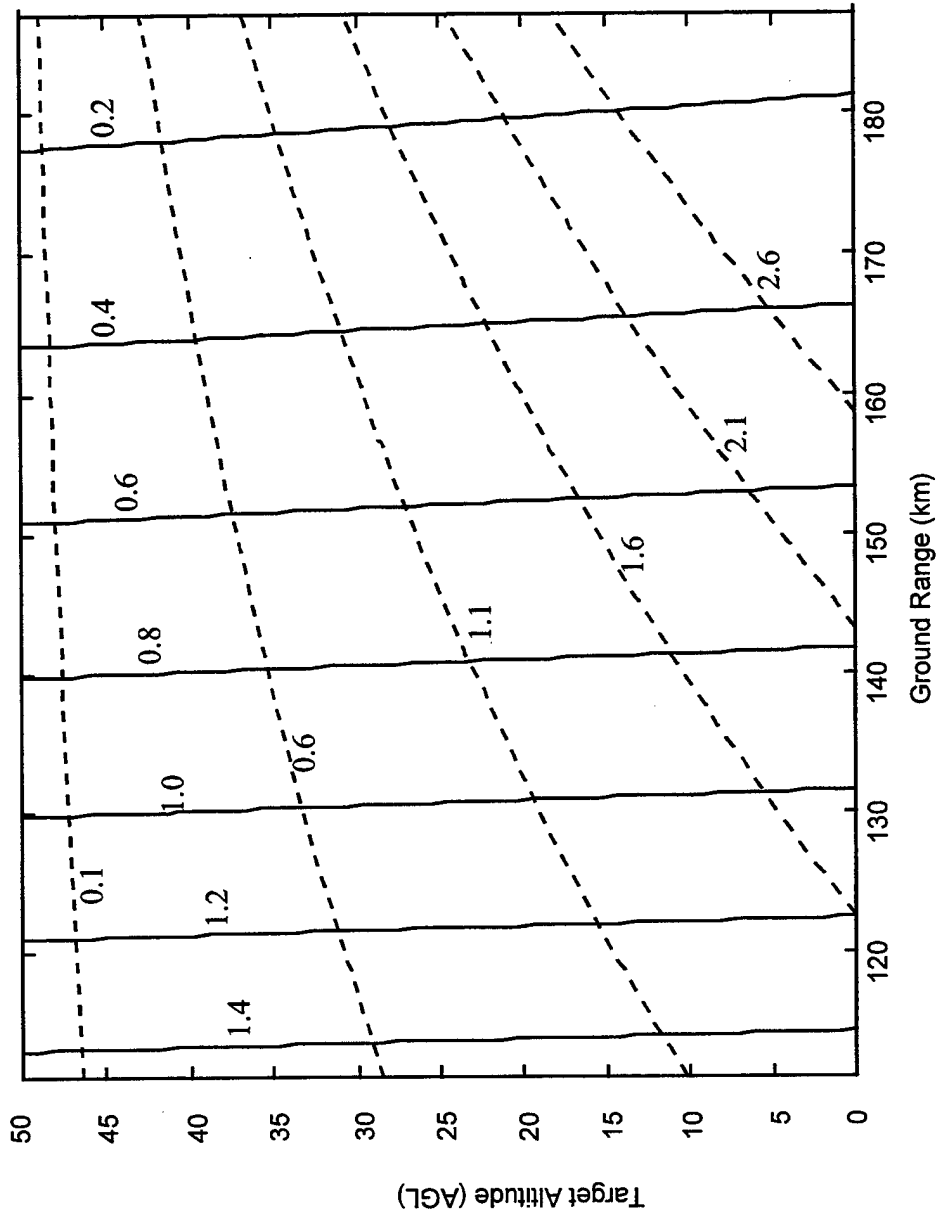


FIGURE 7. APPROACH ANGLES (SOLID LINES) AND PATH LENGTHS (DASHED LINES):
DUCT CEILING OF 50 m AND SENSOR ALTITUDE OF 5000 m

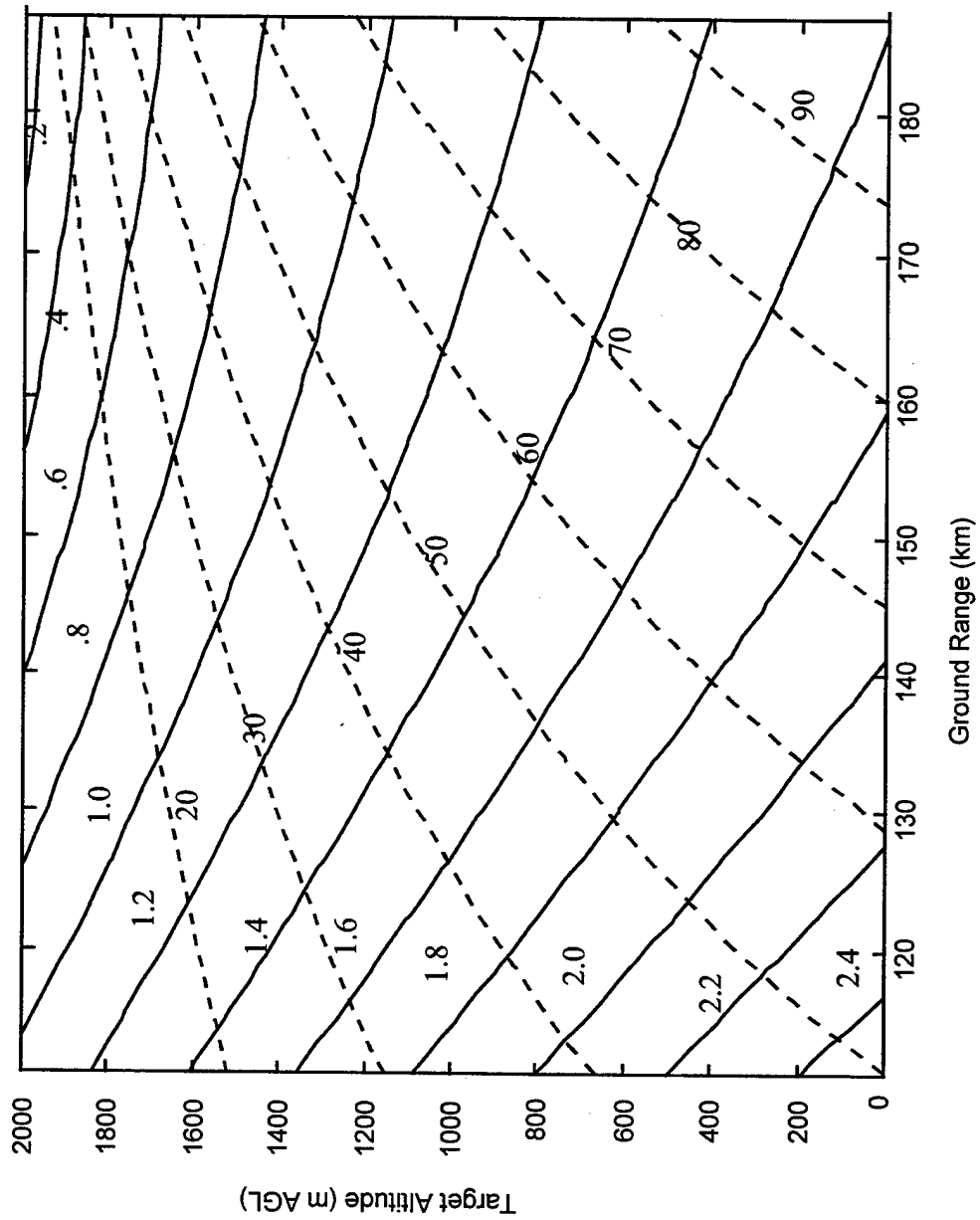


FIGURE 8. APPROACH ANGLES (SOLID LINES) AND PATH LENGTHS (DASHED LINES):
DUCT CEILING OF 2000 m AND SENSOR ALTITUDE OF 5000 m

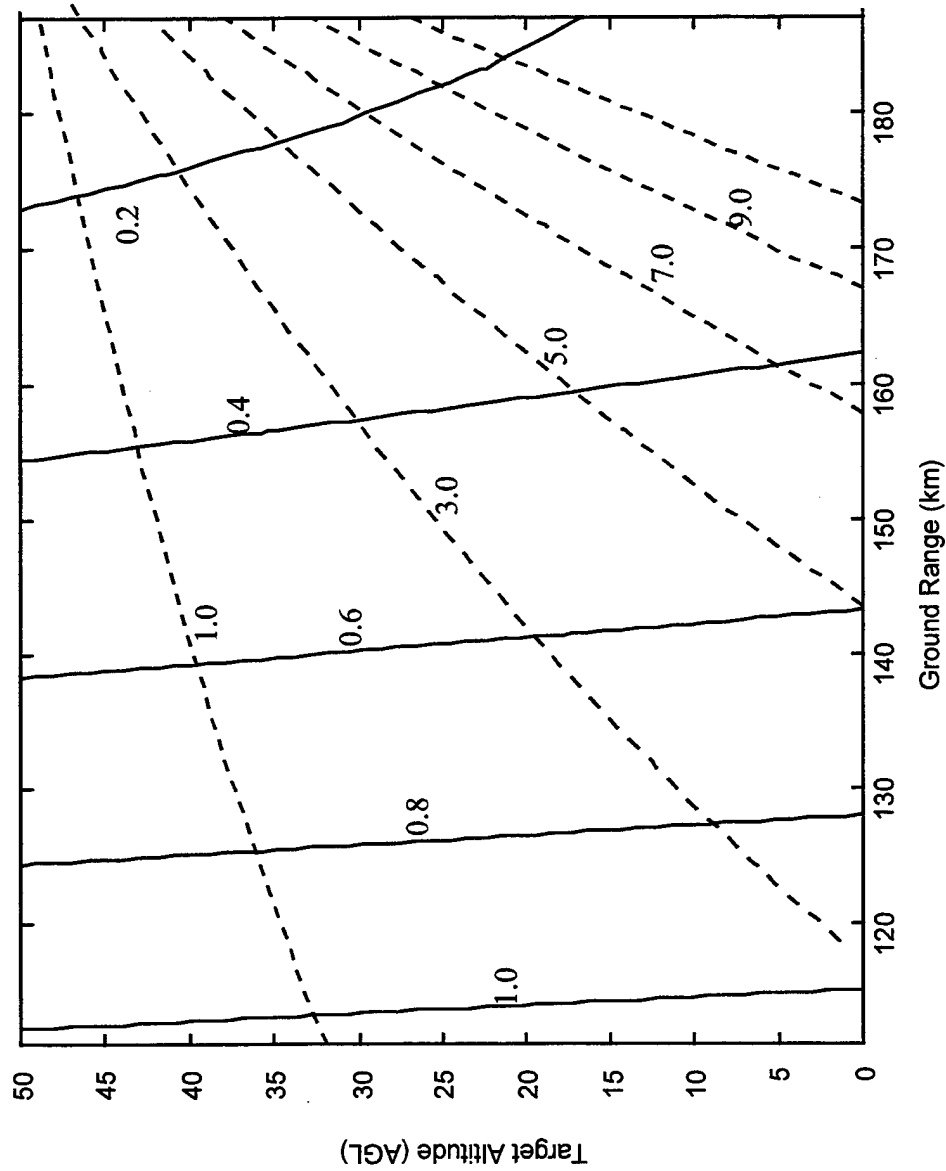


FIGURE 9. APPROACH ANGLES (SOLID LINES) AND PATH LENGTHS (DASHED LINES):
DUCT CEILING OF 50 m AND SENSOR ALTITUDE OF 3000 m

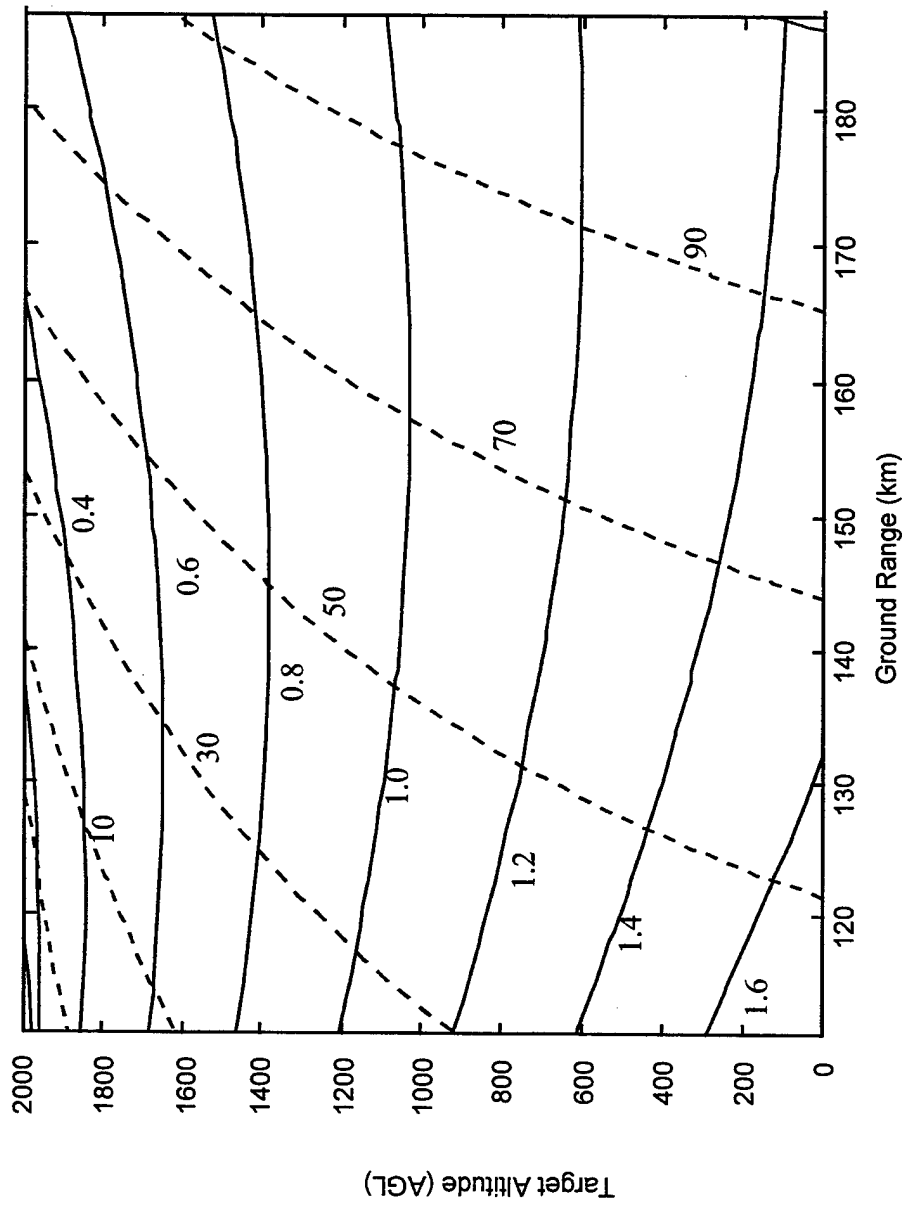


FIGURE 10. APPROACH ANGLES (SOLID LINES) AND PATH LENGTHS (DASHED LINES):
DUCT CEILING OF 2000 m AND SENSOR ALTITUDE OF 3000 m

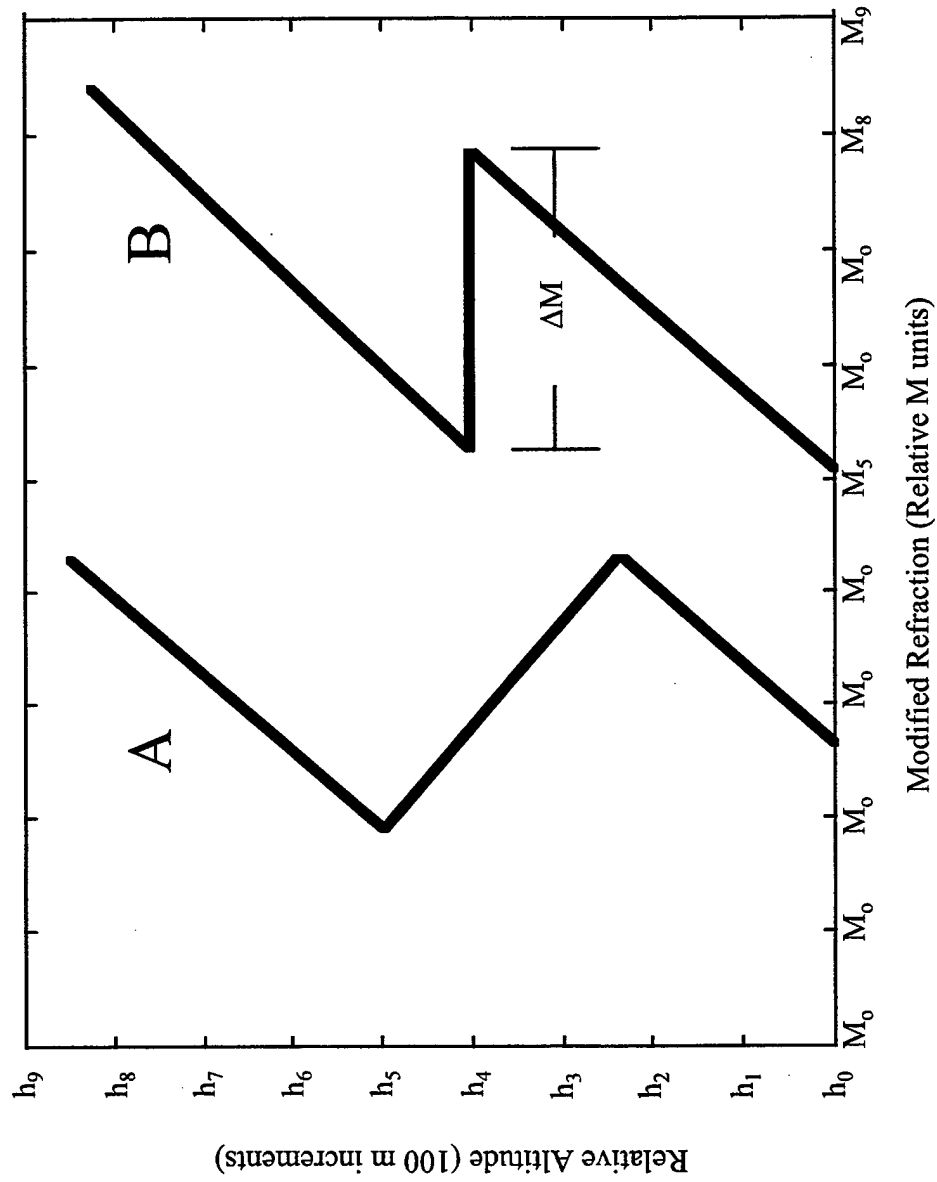


FIGURE 11. MODIFIED REFRACTION PROFILES: "A" IS A REALISTIC PROFILE AND "B" IS AN ALTERED PROFILE USED IN THIS REPORT

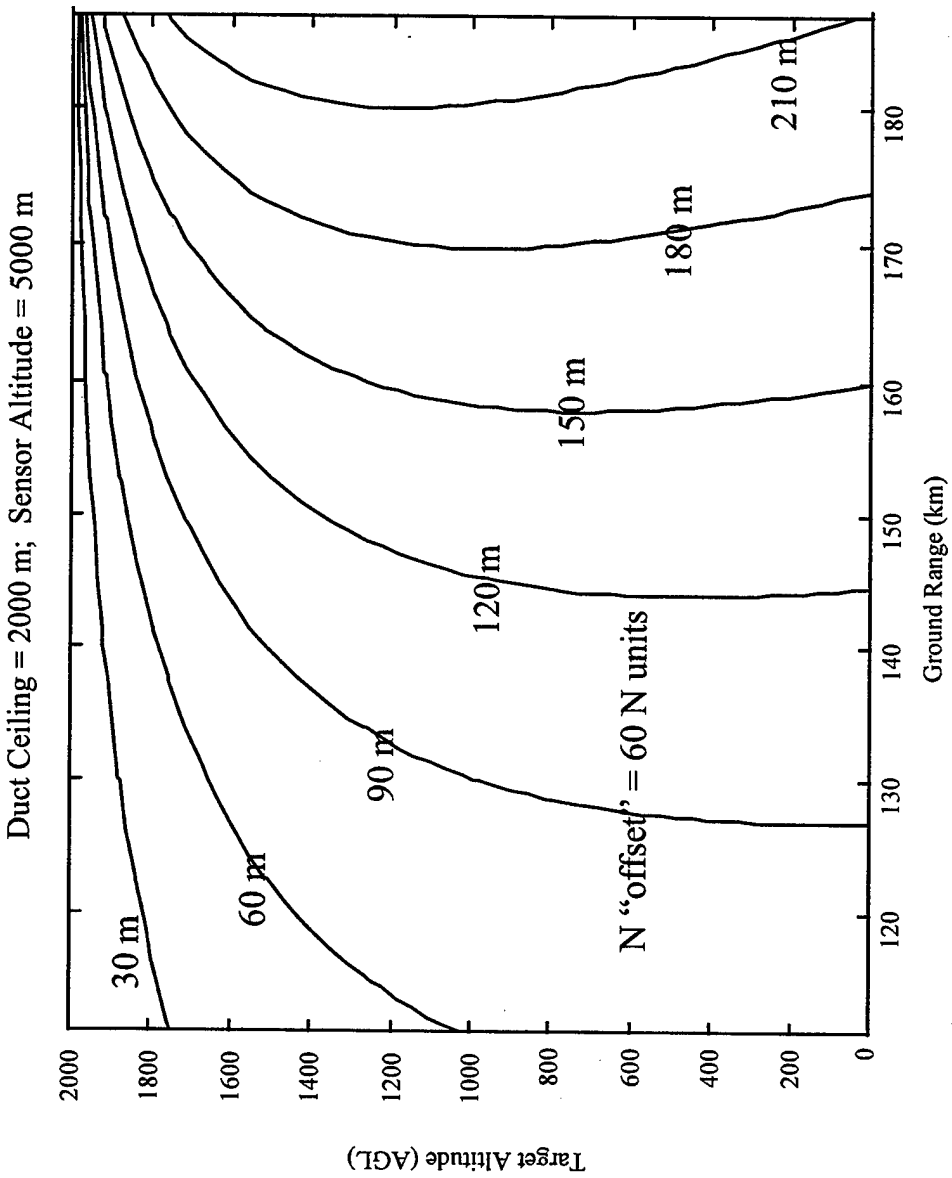


FIGURE 12. VERTICAL POSITION ERRORS INDUCED BY REFRACTION:
N "OFFSET" OF 60 N UNITS

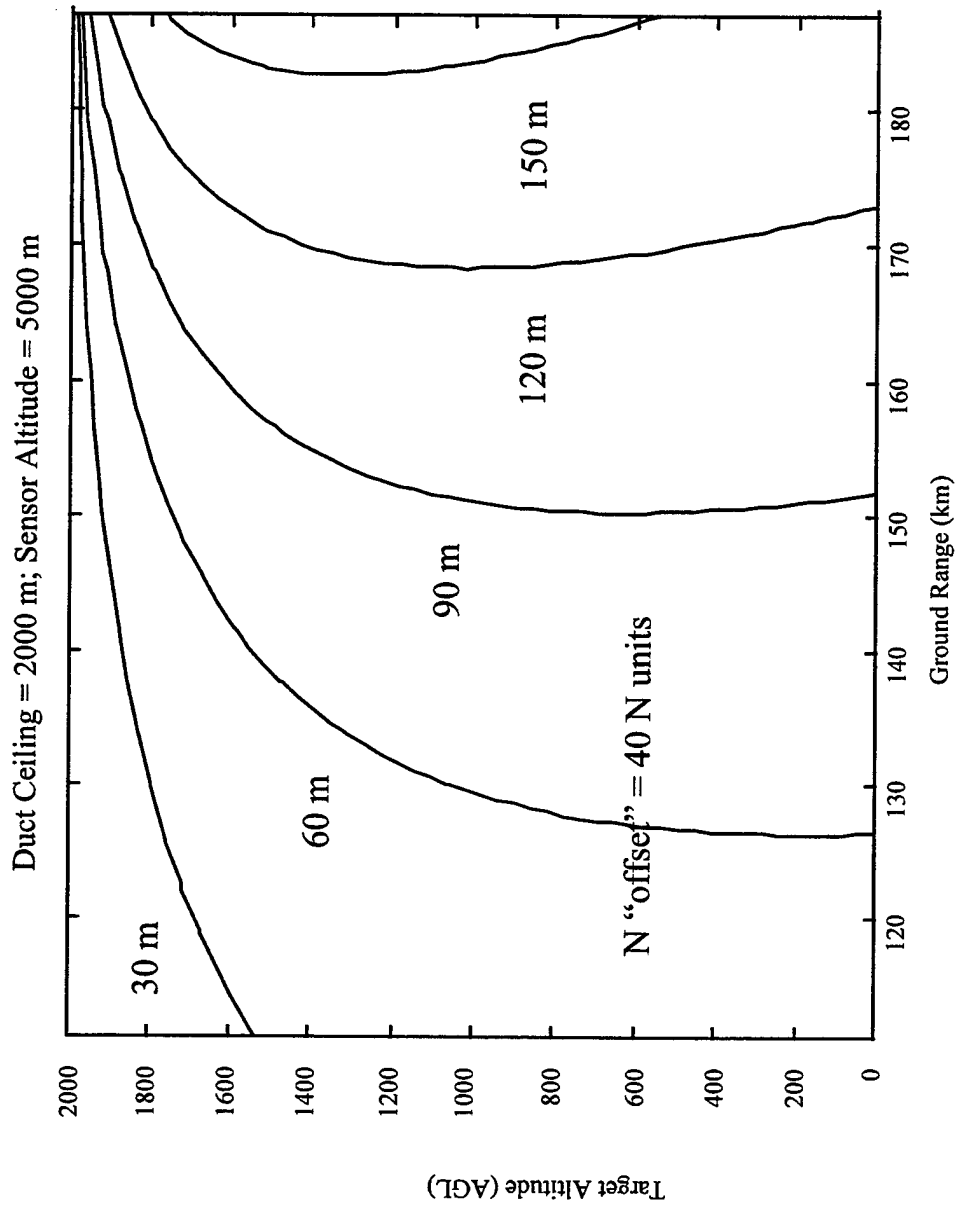


FIGURE 13. VERTICAL POSITION ERRORS INDUCED BY REFRACTION:
N "OFFSET" OF 40 N UNITS

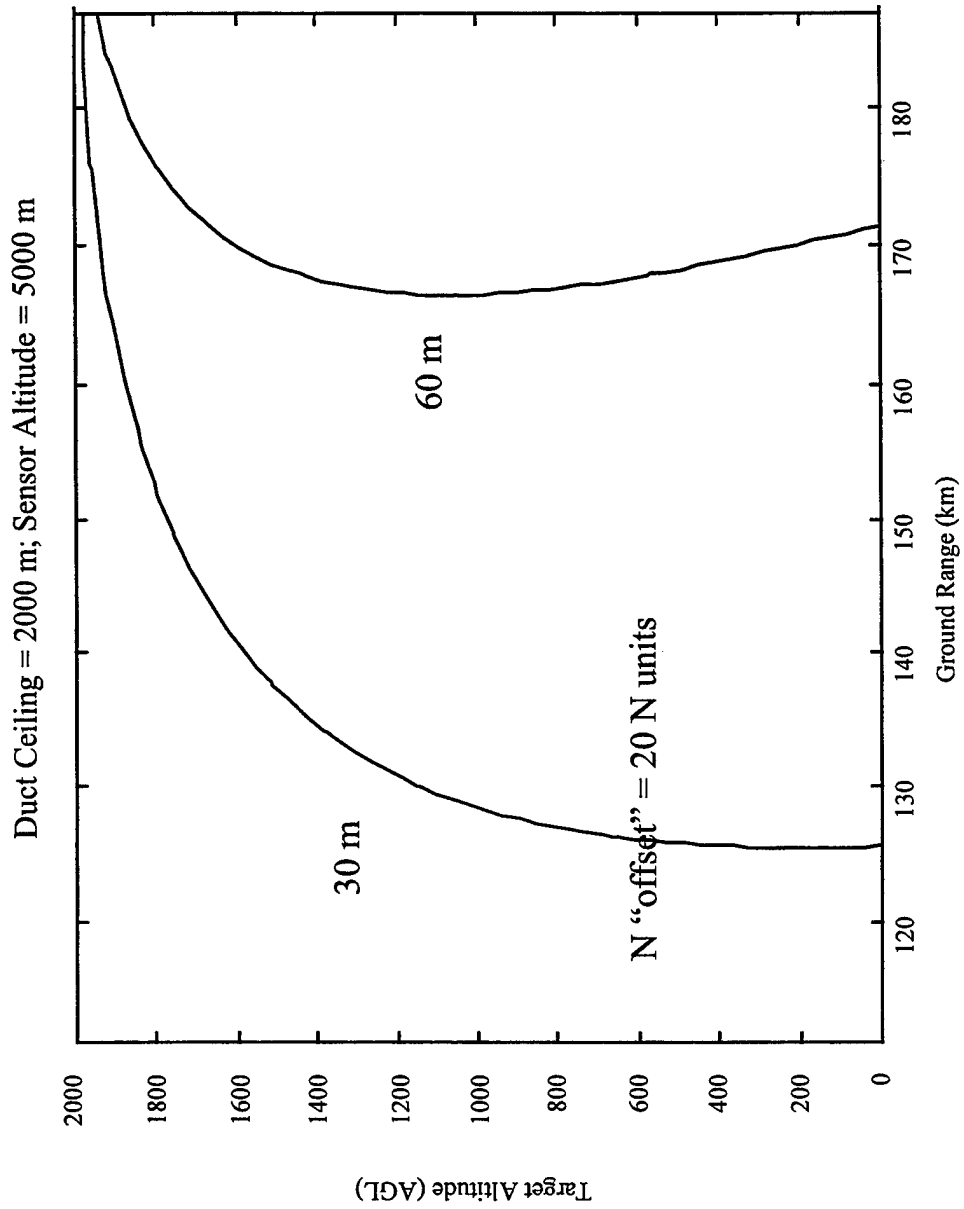


FIGURE 14. VERTICAL POSITION ERRORS INDUCED BY REFRACTION:
N "OFFSET" OF 20 N UNITS

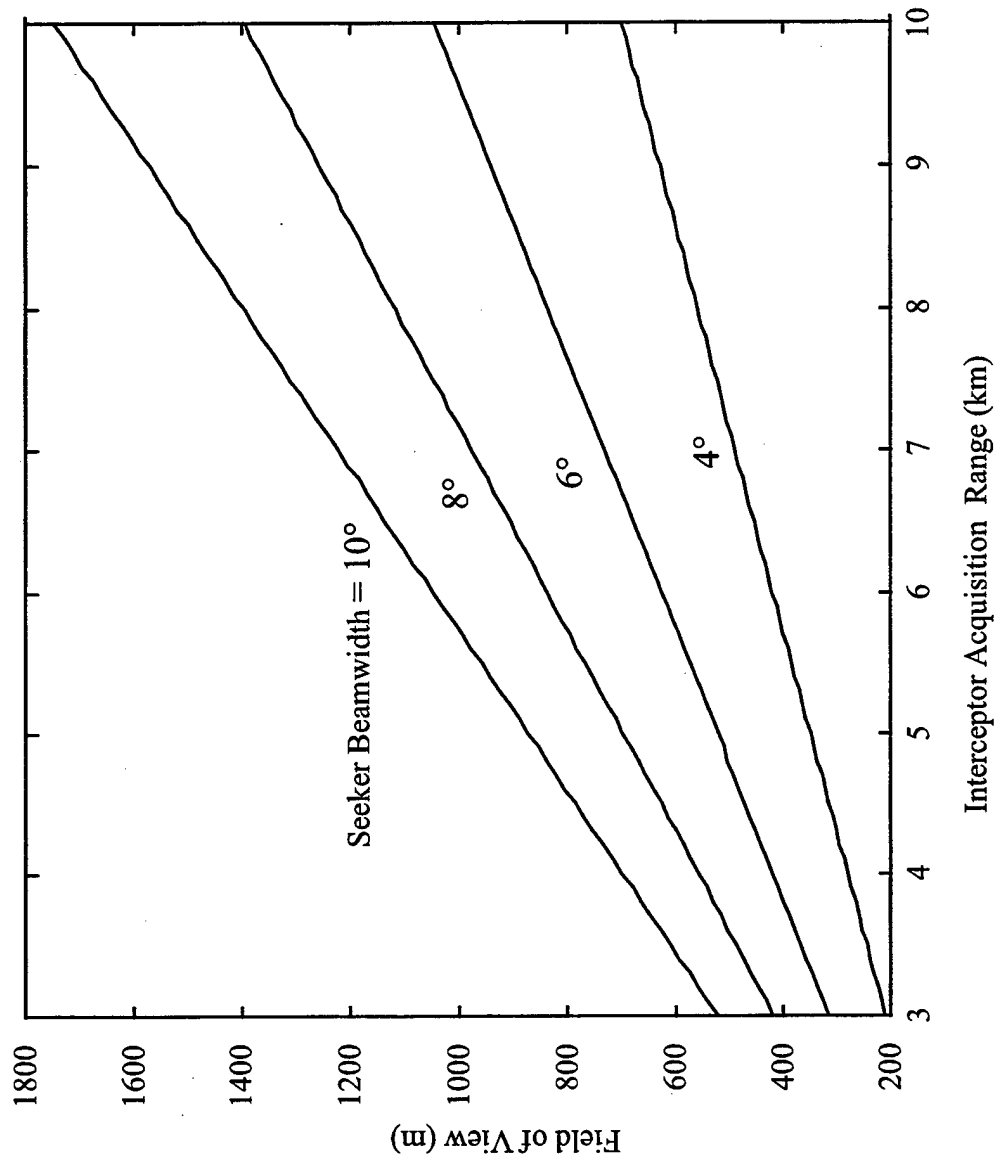


FIGURE 15. INTERCEPTOR SEEKER FIELD OF VIEW

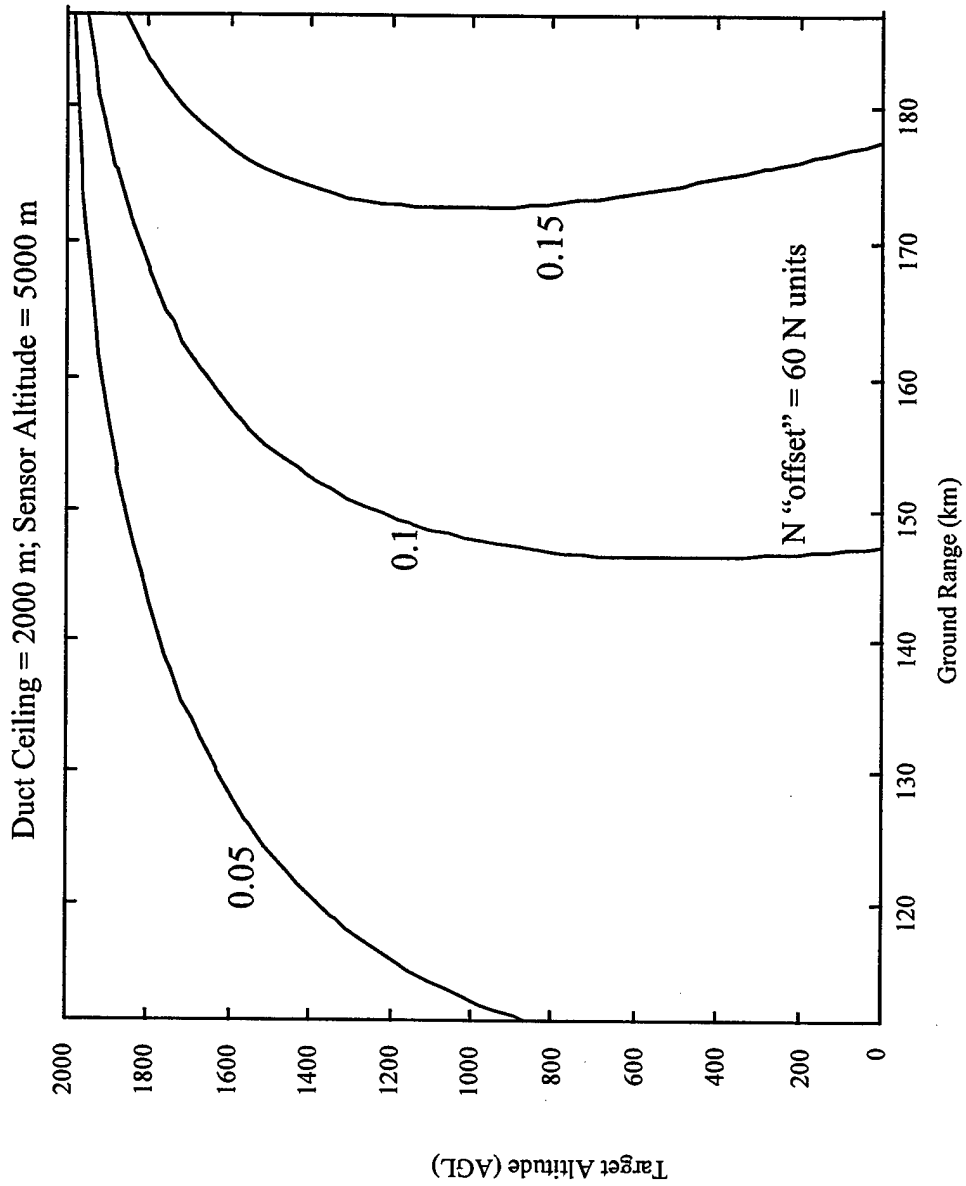


FIGURE 16. RATIO OF ALTITUDE ERRORS TO SEEKER FIELD OF VIEW
(SEEKER BEAMWIDTH = 8°; ACQUISITION RANGE = 9 km)

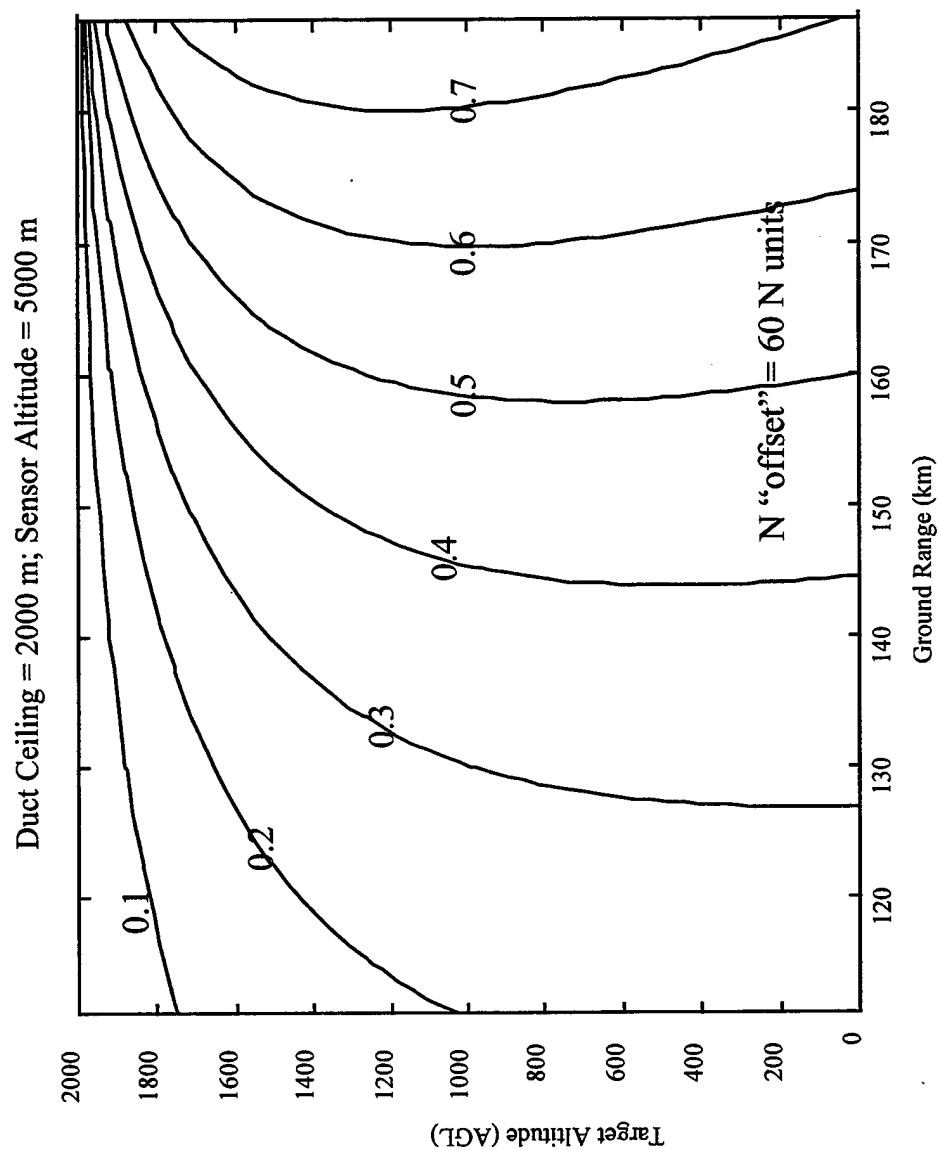


FIGURE 17. RATIO OF ALTITUDE ERRORS TO SEEKER FIELD OF VIEW
(SEEKER BEAMWIDTH = 4°; ACQUISITION RANGE = 5 km)

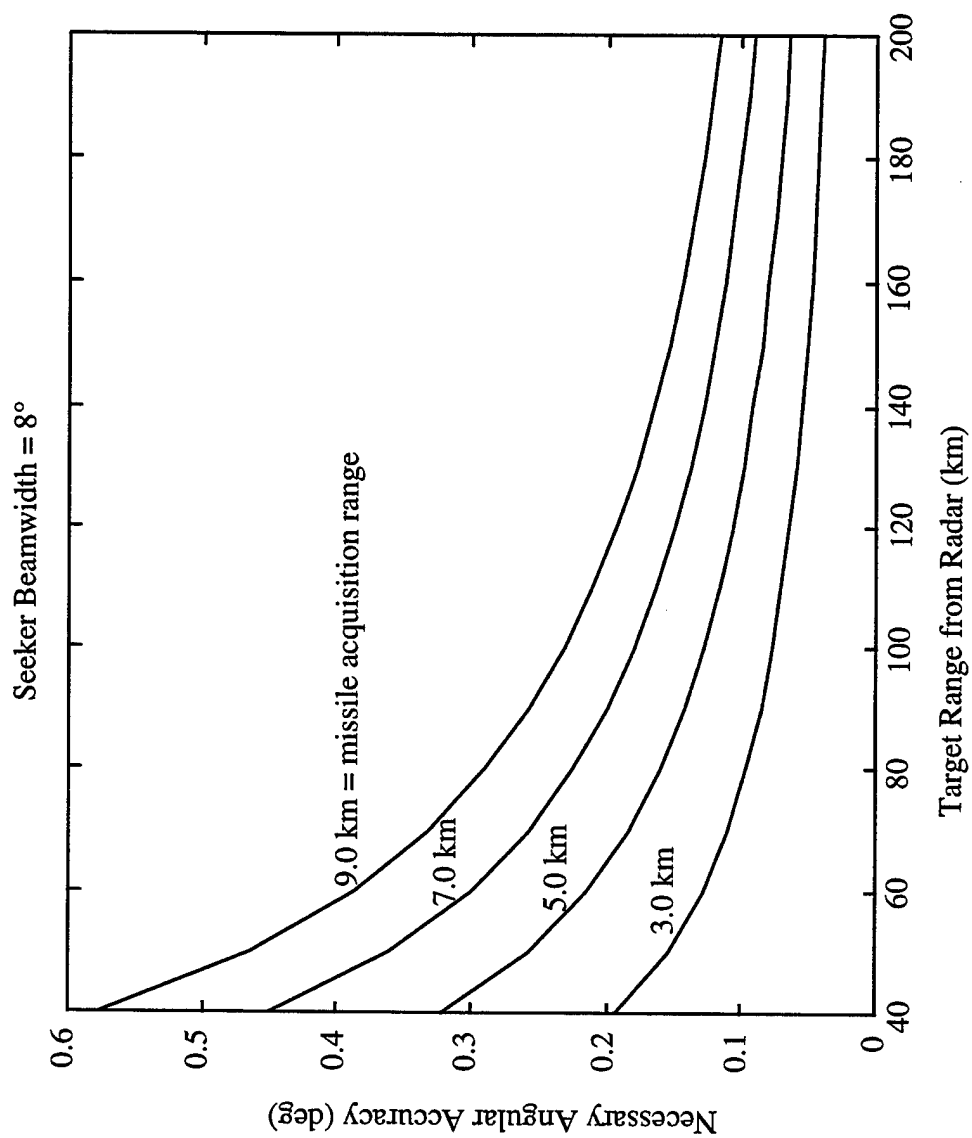


FIGURE 18. SENSOR ANGULAR ACCURACY

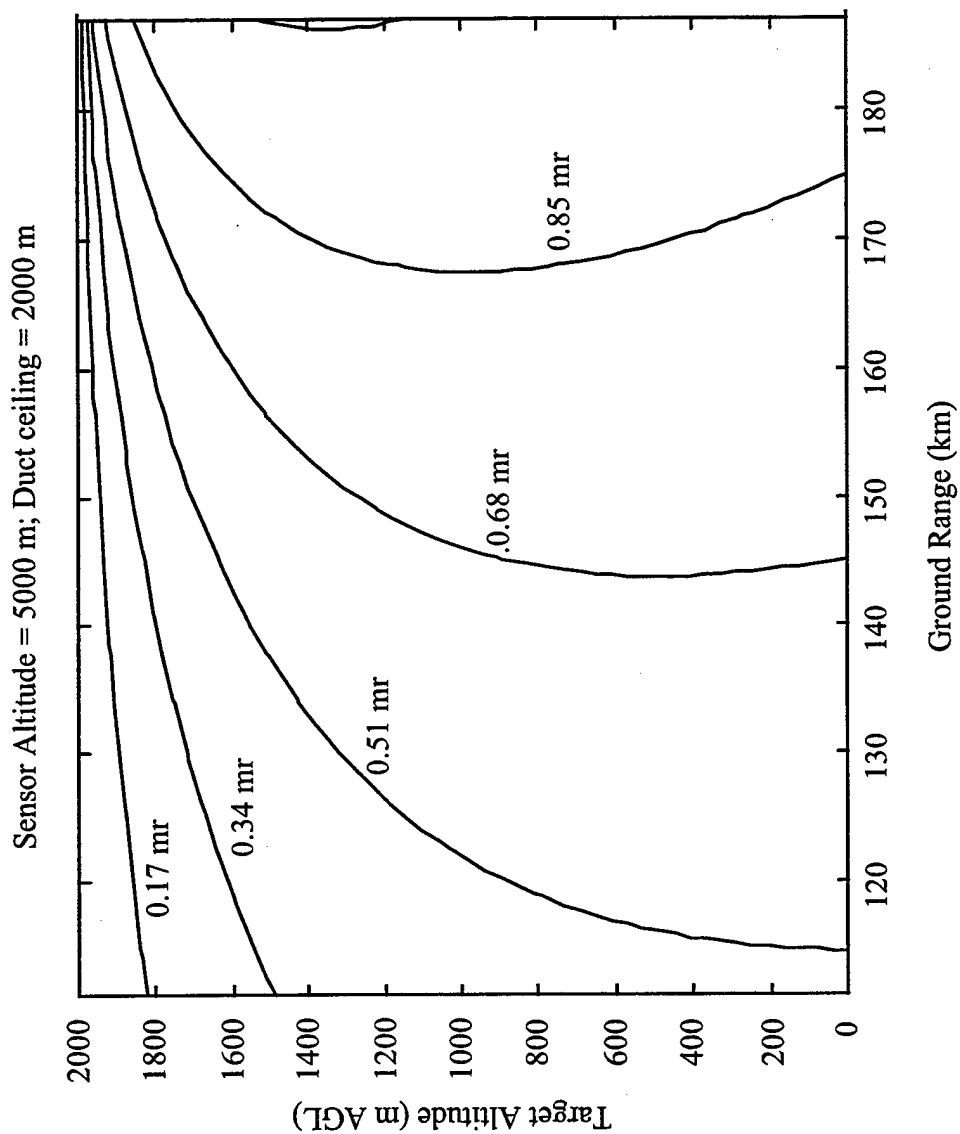


FIGURE 19. ANGULAR ERROR INDUCED BY ATMOSPHERIC REFRACTION

DISTRIBUTION

	<u>Copies</u>		<u>Copies</u>
DOD ACTIVITIES (CONUS)		T42 (STAPLETON)	1
		T44	1
ATTN CODE A76		T50	1
(TECHNICAL LIBRARY)	1		
COMMANDING OFFICER			
CSSDD NSWC			
6703 W HIGHWAY 98			
PANAMA CITY FL 32407-7001			
 DEFENSE TECH INFORMATION CTR			
8725 JOHN J KINGMAN RD			
SUITE 0944			
FORT BELVOIR VA 22060-6218	2		
 NON-DOD ACTIVITIES (CONUS)			
THE CNA CORPORATION			
P O BOX 16268			
ALEXANDRIA VA 22302-0268	1		
 INTERNAL			
B60 (TECHNICAL LIBRARY)	3		
T	1		
T04	1		
T10	1		
T20	1		
T30	1		
T40	1		
T40 (GIORGIS)	1		
T41	1		
T41 (HEADLEY)	1		
T41 (KEENER)	15		
T41 (KIRKPATRICK)	1		
T41 (LIBRARY)	1		
T41 (MORRISSETT)	1		
T41 (OSBORNE)	1		
T41 (PAWLAK)	1		
T41 (SPOONER)	1		
T41 (STAPLETON)	1		
T41 (STUMP)	1		
T41 (WISS)	1		
T42	1		